Dual-Circularly Polarized Single-Element Patch Antenna with Compact Multi-Port Feeding

Dual-Circularly Polarized Single-Element Patch Antenna with Compact Multi-Port Feeding

Mazen Almalki, Bandar Alshammari and Symon K. Podilchak, *Member, IEEE*

***Abstract*—A circularly polarized (CP) S-band patch antenna that makes use of a multi-port setup to improve its radiation efficiency and compactness is presented. The design highlights a single-element patch with eight-port feeding, by using compact slot meandering. To the best knowledge of the authors, no earlier literature discloses a similar single-element patch with eight feeding points made compact by slot meandering whilst demonstrating comparable performances, BW, agility, and polarization purity. In addition, our design utilizes eight, 50-Ω microstrip ports to set and excite the orthogonal polarization states. The miniaturized feeding arrangement, directly under the patch, enables the antenna to produce both left-handed and right-handed CP (as well as other polarization states), making the design suitable for full-duplex and diversity scenarios.**

***Index Terms*—Circular polarization, compactness, multi-port.**

I. Introduction

CIRCULARLY polarized (CP) antennas continue to be of interest, offering advantages of reduced multipath interference and decreased polarization orientation mismatch, making them appealing for wireless and satellite systems [1]. Dual-polarization antennas, providing polarization diversity, are also advantageous for wireless communications in complex environments where direct line of sight is challenging [1]–[6]. Dual-circularly polarized (DCP) antennas, such as those in [6] and [7], can also reduce power consumption for mobile devices and enhance wireless sensor networks, offering benefits like wake-up signals and data transmission. DCP antennas also find utility in satellite systems and geolocation positioning [8], [9].

Switching approaches have also been recently reported for DCP antennas [7], [10]. These methods enable one polarization state to be active when the power level falls below a certain threshold, enhancing link recovery. Similarly, the equal gain combiner (EGC) technique [11] combines signals from desired polarization states. In general, dual-polarization can be achieved by supporting orthogonal field profiles with a single antenna element or by using two orthogonal antennas. The former method is favored, although it can complicate antenna design when DCP functionality is required.

Meeting these requirements involves designing flexible and polarization-diverse antennas, often adopting PCB design techniques when low cost structures are of interest. For example, conventional microstrip patches are preferred for CP and DCP realization due to their cost-effectiveness, low-profile implementation, and high gain radiation properties. Single-feed CP radiation can be achieved by activating two orthogonal patch modes with a 90° phase shift. However, such antennas tend to exhibit narrow impedance matching and limited axial ratio bandwidths (BWs). Additionally, a classic strategy to generate single-CP is by using 90° sequential rotation (SR) in the port phasing using linearly polarized antennas [12]. This approach, whether implemented with a single element or a 2×2 array, can provide enhanced radiation performance, including improved polarization purity, wider AR bandwidths, and symmetrical radiation patterns. The choice among these techniques depends on specific scenario requirements. To generate DCP radiation, branch line coupler feeding [4], [13], [14] can also be adopted, offering two output signals with identical amplitude and the required 90° phase shift. This feeding technique has also been employed to realize dual-linearly polarized radiation [8], [9]. Other DCP configurations have also been explored in [15]–[19].

Advancing upon these recent works and design approaches, this letter proposes a simple and single-element patch antenna (see Figs. 1 to 3, Tables I and II) that can offer simultaneous DCP radiation, low cross-polarization levels, and operational frequency agility for the structure. The unique highlight of this design lies in its miniaturization of eight feeding slots by meandering (having a physical length of about $\lambda/4$), and this arrangement is optimized underneath a single patch radiator achieving compactness and with competitive port isolation. Moreover, this compact meandered slot feeding offers a simple approach to alter the operational frequencies of the antenna.

It should be noted that conventional implementation would require 8 unfolded slots (with electrical lengths slightly less than $\lambda/2$) which would not be possible to similarly position and integrate under a single patch. Also, a 2×2 array could be designed with two feed points per radiator. However, with our newly proposed configuration, a single patch antenna with eight external feeding ports is shown to efficiently generate RHCP or LHCP at desired frequencies. This defines the examined polarization states (see Table I, similar to [8]), other states are possible for diversity applications as required. To the best knowledge of the authors, no similar DCP antenna concept and compact feeding arrangement with miniaturization has ever been documented, employing only a single radiating patch element while offering structural versatility and frequency agility, CP pattern purity, low cross-polarization levels, and competitive 3 dB AR-BW performances. Table III compares other relevant designs outlining these advancements.

II. Antenna Configuration & Design

Figures 1 to 3 depict the structural layout for the DCP patch antenna, while Tables I and II defines the examined polarization states and optimized dimensions. The structure consists of two equally sized substrates: the top uses Rogers

TABLE I
FEED DEFINITIONS AND EXCITATION TO ACHIEVE THE EXAMINED CIRCULAR POLARIZATION STATES (OTHER POLARIZATIONS POSSIBLE)

Polarization	Port 1	Port 2	Port 3	Port 4	Port 5	Port 6	Port 7	Port 8
CP State #1 (RHCP)	$1\angle 0°$	$1\angle -90°$	$1\angle -180°$	$1\angle -270°$	0	0	0	0
CP State #2 (LHCP)	0	0	0	0	$1\angle 0°$	$1\angle +90°$	$1\angle +180°$	$1\angle +270°$

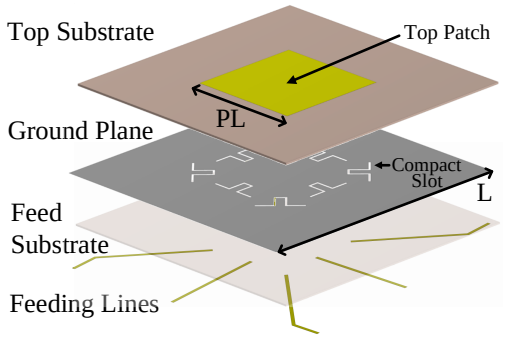

Fig. 1. Perspective view for the single-element design with multi-port feeding.

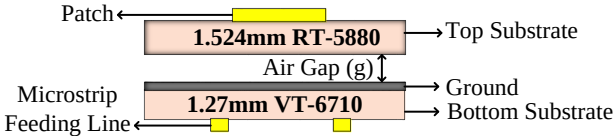

Fig. 2. Cross-sectional view for the proposed multi-port antenna. Note: design features are not to scale, but illustrated here to explain the PCB stack-up.

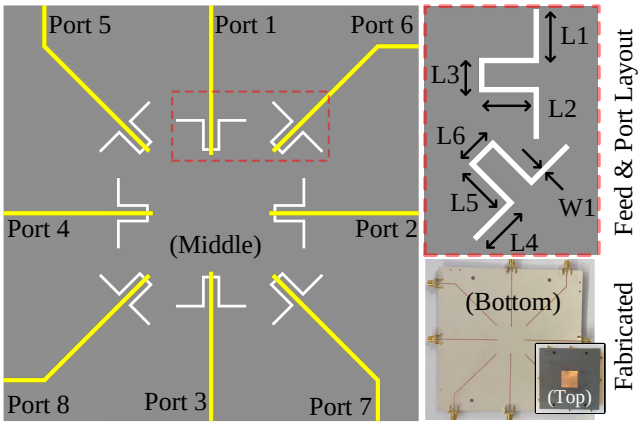

Fig. 3. Compact meandered slot and port layout for the proposed 8-port antenna. The microstrip lines are shown in yellow, the slots in white, and the ground plane in gray. Also shown is the fabricated Design B (bottom-right).

5880 (ϵ_r = 2.2, $\tan\delta$ = 0.0009), and the bottom substrate is defined by ϵ_r = 10.7, $\tan\delta$ = 0.0023 (i.e. VT-6710). The PCB substrate thicknesses are 1.27 mm and 1.524 mm, respectively.

Eight 50-Ω microstrip feeding lines are positioned on the bottom side of the lower layer and all have a width of $W2$. The single radiating patch on the top layer is excited by the compact and meandered slots. In addition, the structure was optimized in a commercial full-wave solver to minimize the coupled power between the eight slots (and external ports), while also aiming for high DCP gain and efficiency as well as reduced cross-polarization. This was made possible by the appropriate positioning of the patch and slots as well as the thickness of the noted air gap g between the substrates.

It should also be mentioned that in our design we aim for polarization purity and best possible AR-BW, and this is achieved by applying a SR approach in phase feeding for the single patch. A more conventional approach would employ a 2×2 array to achieve comparable AR, but this would require additional structure size. To obtain the noted DCP operation, the proposed single-element uses eight feed points by following [8], [9], and as reported in [20]–[22] for more conventional structures, the use of four feed points can help to reduce x-pol. levels and suppress unwanted field configurations (which are related to unwanted higher order modes). Basically, the principle of the newly adopted excitation technique, in our paper, is that a linearly polarized element (a single-element square patch, in our case) can generate DCP, in particular, by driving the sides or four corners of the patch with equal power and 90° phase differences for RHCP or LHCP (see Table I).

The eight ports have been placed to achieve these DCP states, for example, ports 1 to 4 define the first CP state; i.e. CP1. Similarly, ports 5 to 8 for CP2. It is also possible to interchange the phase to achieve the opposite polarization; i.e. RHCP for ports 1 to 4 and LHCP for ports 5 to 8. The patch feeding arrangement can also accommodate for various linear polarization states, depending on the specific polarization diversity requirements, and, in addition to RHCP and LHCP. More specifically, the design can support a comprehensive set of polarization states, including vertical (V) polarization, horizontal (H) polarization, linear polarization at +45 degrees (L45), and, linear polarization at -45 degrees (L-45). These polarization options provide versatility making the design suitable for various polarization diverse scenarios as required.

It should also be noted that this letter advances from earlier findings by some of the authors in [23], in particular, where preliminary results using H-shaped slots were reported. This created a wide operational BW for one CP state. However, because of the high coupling in that design by the noted slot configuration [23], which increased to beyond -5 dB, antenna efficiency was diminished to below 65% and gain for one CP state was only about 2.5 dBic. These design features make selective frequency operation not very practical for the two CP states. While the more wideband design, [23], has the benefits of sensing across a large frequency range for one CP state, it also has the downside of possibly greater power consumption and interference, particularly when both CP states occupy the same frequency band. More narrowband features, on the other hand and as proposed in this letter, offers some advantages such as requiring narrower BWs for the signals and this can simplify transceiver hardware. This also eliminates the need for extra components such as (narrowband) bandpass filters.

TABLE II
STRUCTURE DIMENSIONS (VALUES IN MILLIMETERS, SEE FIGS. 1 TO 3)

	L1	L2	L3	L4	L5	L6	g	W1	PL
Values	7.1	7.1	3	6.62	6.62	3	10	0.5	41

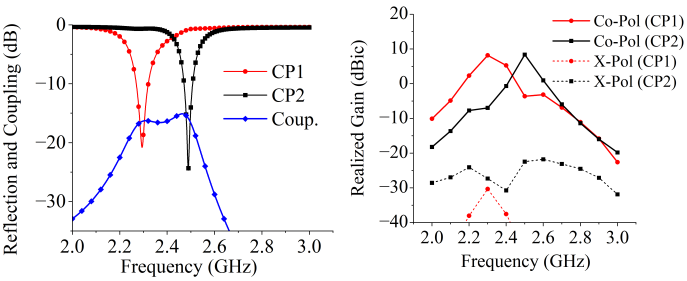

(a) F-Parameters (b) Realized Gains

Fig. 4. The simulated active reflection and coupling coefficients (or F-parameters from CST) at Ports 1 and 5 when 90° SR is applied for CP1 and CP2, respectively. Analogous results were observed for the other ports.

III. Design Results & Discussions

The structure was optimized using CST Microwave Studio, and the simulations are reported in Figs. 4 to 7. The active reflection coefficients, also known as F-Parameters in CST, are presented in Fig. 4(a). For the proposed design, two distinct resonant frequencies can be obtained, depending on the four middle-meandered slot lengths. For CP1, the resonant frequency spans from 2.27 to 2.32 GHz, while the resonant frequency for CP2 ranges from 2.47 to 2.51 GHz, primarily defined by the length of the corner slots. Additionally, Fig. 4(b) illustrates the simulations for gain, demonstrating high CP purity due to the low cross-polarization levels.

Given that the meandered slot lengths (see Table II) can be selected prior to the PCB manufacturing stage, the structure has the capability to tune the frequency for best matching while keeping the other operational frequency stationary (see Fig. 5). This flexibility makes the design suitable for agile frequency systems, and some applications include transceivers requiring adjacent frequency bands [24]–[28]. Moreover, Fig. 5(a) reports a parametric study for some of the possible reflection coefficients, while Fig. 5(b) shows the realized gain.

These results demonstrate the versatility in the structure, in that by changing $L4$ and $L5$, the operational frequency can be altered. Specifically, the design frequency and peak gain of the upper band can increase from approximately 2.4 GHz to 2.6 GHz, and by only changing the corner meandered slot lengths while maintaining patch size and all other structure parameters. In addition, the lower-band remains unaffected by these length variations and similarly when adjusting $L1$ and $L2$, resulting in a corresponding change in the lower band (all results not reported for brevity). By this simple variation of the structure parameters for the meandered slot lengths, we can achieve control of the frequency ratio (FR) from about 1.0 to 1.25 for the distinct CP bands.

To illustrate the profiles for the polarization states CP1 and CP2, the surface current distributions were simulated and reported as shown in Fig. 6. Also, the electric field was simulated and minimal power was observed to be coupled to ports 5 to 8, when ports 1 to 4 were driven for CP1 (similarly for CP2, and all results not shown for brevity). These results were consistent with the low coupling values of -15 dB (or lower) as reported in Fig. 4(a). It should also be mentioned that a single-layer design (no air gap) was initially

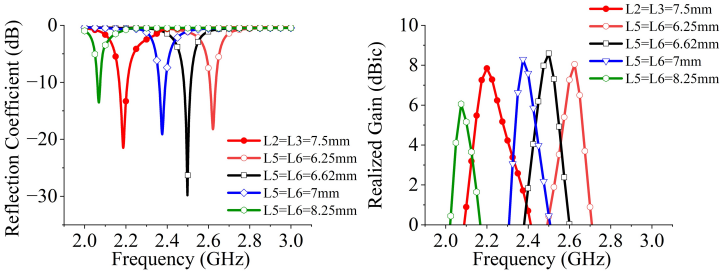

(a) Reflection Coefficients (b) Realized Gains

Fig. 5. Simulation study for the passive reflection coefficient and peak gain.

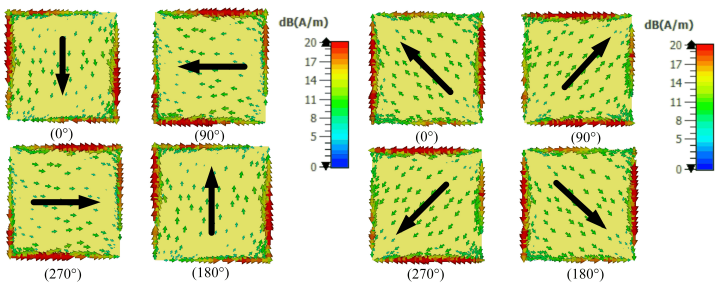

(a) Ports 1 to 4 Driven for CP1 (b) Ports 5 to 8 Driven for CP2

Fig. 6. The surface currents on the top patch for both polarization states.

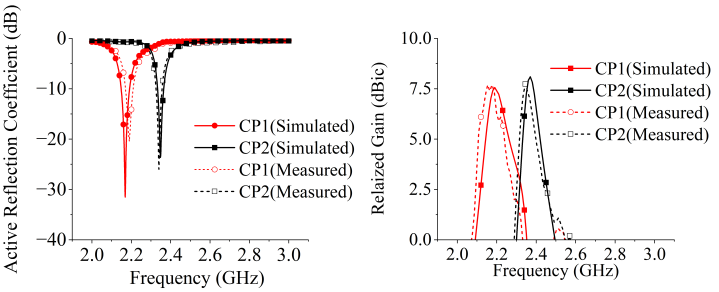

(a) Reflection Coefficients (b) Realized Gains

Fig. 7. Simulated and measured active reflection coefficient and peak gain.

designed for comparison to the proposed multi-layer structure, but the coupling values were more than -5 dB (all results not reported). This is because as in the proposed multi-layer design, the distance between the feeding slots and the top patch is increased (by about 10 mm due to the air gap, see Table II) and hence coupling values can be reduced. In addition, this multi-layer approach can also enhance the BW as per the aforementioned design motivations.

IV. Experimental Results

The multi-port patch was fabricated to experimentally verify the antenna concept. Bottom and top view photographs for the prototype are shown in Fig. 3 (see bottom-right inset). In addition, the two PCB layers were affixed using plastic fastners. In Fig. 7(a), it can be noticed that the port matching is very comparable, making simulations and measurements in good agreement. Radiation characteristics, port coupling, beam patterns, and ARs are reported in Figs. 7(b) to 10.

For the far-field studies, measurements were completed in a calibrated anechoic chamber and external 90° and 180° couplers were employed to feed the antenna under test to excite the noted CP states. In addition, the losses from the

TABLE III
PERFORMANCE COMPARISONS AMONG OTHER RELEVANT DUAL-BAND & DUAL-CIRCULARLY POLARIZED PATCH ANTENNA DESIGNS

	-10 dB Matching Frequency Range (GHz)	Frequency Ratio	3dB AR Bandwidth	Structure Symmetry (YES/NO)	X-Pol. Level Below Beam Peak (dB)	Lowest Freq. Size ($/\lambda_0$)	CP Max Gain (dBic)	Peak Eff.	Single Element or Array
[24]	CP1: 2.38 to 2.46 CP2: 2.64 to 2.71	1.12	0.9% 0.3%	NO	-18.6, -14.5	1.4×1.4×0.027	11.8	-	Array (2×2)
[25]	CP1: 2.48 to 2.57 CP2: 3.57 to 3.69	1.42	0.7% 0.6%	NO	-18.5, -17.2	1.2×1.2×0.027	12.5	-	Array (2×2)
[26]	CP1: 1.60 to 1.63 CP2: 2.40 to 2.57	1.55	0.6% 1.4%	NO	-	∼0.4×0.4×0.08	6.4	-	Element
[27]	CP1: 2.13 to 2.15 CP2: 2.17 to 2.24	1.04	0.3% 0.7%	NO	-13.1, -15	0.8×0.8×0.02	7.5	85%	Element
[28]	CP1: 2.39 to 2.40 CP2: 2.48 to 2.50	1.04	0.3% 0.7%	NO	-12, -13	0.44×0.48×0.03	5.7	-	Element
Proposed	CP1: 2.17 to 2.21 CP2: 2.35 to 2.38	1.0 to 1.25 (possible)	2.8% 5.0%	YES	-18.8, -25.7	1.1×1.1×0.09	7.7	82%	Element

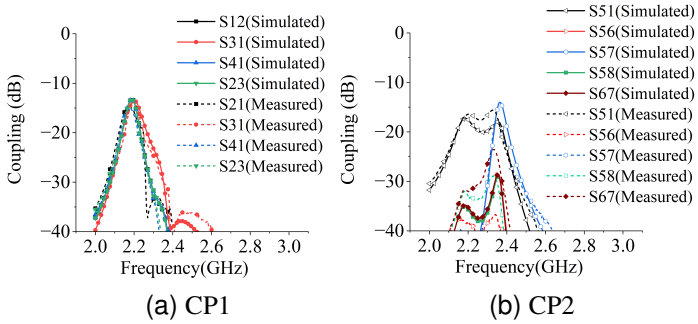

Fig. 8. Simulated and measured passive coupling values between the ports.

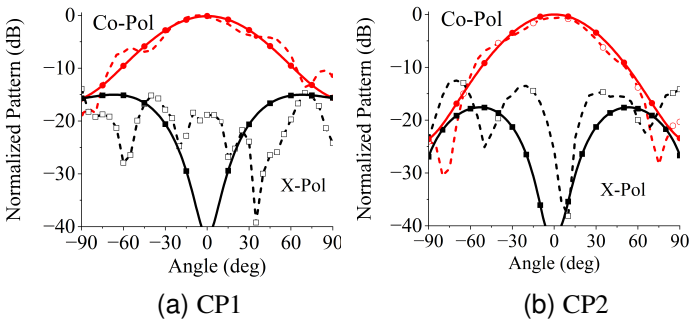

Fig. 9. The simulated and measured CP1 and CP2 normalized beam patterns.

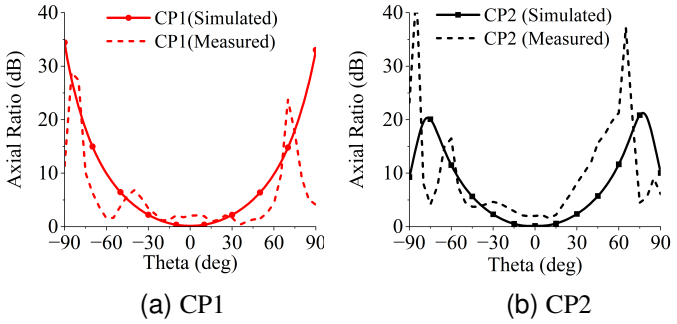

Fig. 10. The simulated and measured AR versus angle for CP1 and CP2.

couplers and the relevant cables were tested and findings were utilized for determination of the measured CP gain. The minor variations between the results can be mainly attributed to practical tolerances for the substrates and antenna fabrication.

Broadside gain results as a function of frequency are shown in Fig. 7(b). As can be observed, the measured gains are in good agreement with the simulations. Maximum values are 7.69 dBic for CP1 at 2.15 GHz and 7.73 dBic for CP2 at 2.34 GHz. S-parameter coupling studies are shown in Fig. 8, and levels are about -15 dB or below. Also, Figs. 9 and 10 report the beam patterns and AR demonstrating good CP purity for the two states, mainly due to structure symmetry.

A comparison between the proposed DCP design with other relevant patch antennas and arrays [24]–[28] is shown in Table III. Our proposed design offers a competitive frequency ratio (FR) ranging from 1.0 to 1.25, a wide 3dB axial ratio bandwidth (AR-BW), and low cross-polarization (X-pol.) levels measuring approximately -20 dB or lower (see Fig. 5 and Table III). As can be observed, no other structure offers comparable BWs, polarization purity, and efficiency. In addition, the radiation performances for the proposed design are achieved while maintaining a low-profile and compact size, whilst employing a single radiating patch element due to the miniaturized feeding slots. To the best of our knowledge, no similar antenna structure has been reported previously.

V. CONCLUSION

An eight-port DCP antenna featuring a symmetric arrangement of meandered slots was presented. By dedicating four slots to each CP state, the single-element patch achieves DCP radiation with high polarization purity. In addition, a prototype has been successfully manufactured, which demonstrates good agreement with the simulations. The design can also enable other polarization states for diversity applications.

Future work can explore the inclusion of an integrated feeding circuit (following [9]) and methods to broaden the BW. Moreover, the proposed single-patch design can be a potential candidate in new array configurations where polarization diversity and CP beam-steering are of interest, leading to enhanced wireless communications and satellite systems. Other potential applications include full-duplex systems or transceivers supporting LHCP or RHCP signals.

ACKNOWLEDGMENTS

The authors would like to thank Maksim Kuznetcov, Zain Shafiq, Iram Shahzadi and Alexander Don for their assistance during fabrication and the measurement setup. Also, The authors thankfully acknowledge the PhD funding support from King Abdulaziz City for Science and Technology (KACST). For the purpose of open access, the author has applied a Creative Commons Attribution (CC BY) licence to any Author Accepted Manuscript version arising from this submission.

REFERENCES

[1] S. S. Gao, Q. Luo, and F. Zhu, *Introduction to circularly polarized antennas*. Wiley-IEEE Press, 2014.

[2] J. Moon and Y. Kim, "Antenna diversity strengthens wireless lans," *Communication Systems Design*, vol. 9, no. 1, pp. 14–24, 2003.

[3] S. K. Yoo, S. L. Cotton, and W. G. Scanlon, "Switched diversity techniques for indoor off-body communication channels: An experimental analysis and modeling," *IEEE Transactions on Antennas and Propagation*, vol. 64, no. 7, pp. 3201–3206, 2016.

[4] C. Zhang, X. Liang, X. Bai, J. Geng, and R. Jin, "A broadband dual circularly polarized patch antenna with wide beamwidth," *IEEE antennas and wireless propagation letters*, vol. 13, pp. 1457–1460, 2014.

[5] P. Xu, Z.-H. Yan, T.-L. Zhang, and X.-Q. Yang, "Broadband circularly polarized slot antenna array using a compact sequential-phase feeding network," *Progress In Electromagnetics Research C*, vol. 47, pp. 173–179, 2014.

[6] T. Kumberg, R. Tannhaeuser, and L. M. Reindl, "Wake-up receiver with equal-gain antenna diversity," *Sensors*, vol. 17, no. 9, p. 1961, 2017.

[7] S. K. Yoo, S. L. Cotton, and W. G. Scanlon, "Switched diversity techniques for indoor off-body communication channels: An experimental analysis and modeling," *IEEE Trans. on Antennas and Propagation*, vol. 64, no. 7, pp. 3201–3206, 2016.

[8] M. V. Kuznetcov, S. K. Podilchak, M. Clénet, and Y. M. M. Antar, "Hybrid dielectric resonator antenna for diversity applications with linear or circular polarization," *IEEE Trans. on Antennas and Propagation*, vol. 69, no. 8, pp. 4457–4465, 2021.

[9] M. V. Kuznetcov, S. K. Podilchak, J. C. Johnstone, M. Clénet, and Y. M. M. Antar, "Planar feeding circuit integrated with a compact dielectric resonator for polarization diversity," *IEEE Trans. on Microwave Theory and Techniques*, vol. 69, no. 4, pp. 2229–2240, 2021.

[10] F. Yang and Y. Rahmat-Samii, "A reconfigurable patch antenna using switchable slots for circular polarization diversity," *IEEE Microwave and Wireless Components Letters*, vol. 12, no. 3, pp. 96–98, 2002.

[11] S. S. Ikki and M. H. Ahmed, "Performance of cooperative diversity using equal gain combining (EGC) over nakagami-m fading channels," *IEEE Transactions on Wireless Communications*, vol. 8, no. 2, pp. 557–562, 2009.

[12] R. Garg, P. Bhartia, I. Bahl, and A. Ittipiboon, *Microstrip Antenna Design Handbook*. Norwood, MA: Artech House, 2001.

[13] A. Benouakta, F. Ferrero, L. Lizzi, and R. Staraj, "Frequency reconfigurable and circularly polarized patch antenna over dual ultra-wideband channels," in *2022 16th European Conference on Antennas and Propagation (EuCAP)*, pp. 1–5, 2022.

[14] V. S. Joshi, B. J. Makwana, and A. M. Kothari, "A circularly polarized dual-band patch antenna with branch-line coupler for irnss application," in *2017 2nd IEEE International Conference on Recent Trends in Electronics, Information Communication Technology (RTEICT)*, pp. 1612–1614, 2017.

[15] H. Alsuraisry, H.-C. Lu, and T.-W. Huang, "A design of circular polarization antenna array using sequential rotation for satcom," in *2021 International Symp. on Antennas and Propagation (ISAP)*, pp. 1–2, IEEE, 2021.

[16] A. Chen, Y. Zhang, Z. Chen, and C. Yang, "Development of a Ka-band wideband circularly polarized 64-element microstrip antenna array with double application of the sequential rotation feeding technique," *IEEE Antennas and Wireless Prop. Letts.*, vol. 10, pp. 1270–1273, 2011.

[17] F. Kurniawan, J. T. S. Sumantyo, F. Oktafiani, G. S. Prabwo, and A. Munir, "A 2×2 X-band array antenna with sequential rotation network feeding for communication," in *2019 IEEE Conf. on Antenna Measurements Applications (CAMA)*, pp. 45–48, 2019.

[18] W. Wang, S. Yang, Z. Fang, Q. Sun, Y. Chen, and Y. Zheng, "Compact dual-polarized wideband antenna with dual-/single-band shifting for microbase station applications," *IEEE Transactions on Antennas and Propagation*, vol. 69, no. 11, pp. 7323–7332, 2021.

[19] S.-K. Lin and Y.-C. Lin, "A compact sequential-phase feed using uniform transmission lines for circularly polarized sequential-rotation arrays," *IEEE Transactions on Antennas and Propagation*, vol. 59, no. 7, pp. 2721–2724, 2011.

[20] H. Wong and W. Lin, "Circularly-polarized conical-beam patch antenna with wide bandwidth and polarization diversity," in *2014 International Symposium on Antennas and Propagation Conf. Proceedings*, pp. 429–430, 2014.

[21] C. E. Santosa and J. T. S. Sumantyo, "Design of broadband X-band subarray antenna with hybrid-sequential rotation fed for airborne CP-SAR," in *2021 7th Asia-Pacific Con. on Synthetic Aperture Radar (APSAR)*, pp. 1–4, IEEE, 2021.

[22] P. Hall, "Design principles of sequentially fed, wide bandwidth, circularly polarised microstrip antennas," *IEE Proceedings H (Microwaves, Antennas and Propagation)*, vol. 136, pp. 381–389(8), October 1989.

[23] M. Almalki, M. V. Kuznetcov, and S. K. Podilchak, "Single-element patch antenna with multi-port feeding for dual-circularly polarized radiation," in *2023 17th European Conference on Antennas and Propagation (EuCAP)*, pp. 1–5, 2023.

[24] Q.-S. Wu, X. Zhang, L. Zhu, J. Wang, G. Zhang, and C.-B. Guo, "A single-layer dual-band dual-sense circularly polarized patch antenna array with small frequency ratio," *IEEE Transactions on Antennas and Propagation*, vol. 70, no. 4, pp. 2668–2675, 2021.

[25] J.-D. Zhang, L. Zhu, N.-W. Liu, and W. Wu, "Dual-band and dual-circularly polarized single-layer microstrip array based on multiresonant modes," *IEEE Transactions on Antennas and Propagation*, vol. 65, no. 3, pp. 1428–1433, 2017.

[26] K. Chen, J. Yuan, and X. Luo, "Compact dual-band dual circularly polarised annular-ring patch antenna for beidou navigation satellite system application," *IET Microwaves, Antennas & Propagation*, vol. 11, no. 8, pp. 1079–1085, 2017.

[27] N.-W. Liu, L. Zhu, Z.-X. Liu, Z.-Y. Zhang, and G. Fu, "Frequency-ratio reduction of a low-profile dual-band dual-circularly polarized patch antenna under triple resonance," *IEEE Antennas and Wireless Propagation Letters*, vol. 19, no. 10, pp. 1689–1693, 2020.

[28] Z. Zhao, F. Liu, J. Ren, Y. Liu, and Y. Yin, "Dual-sense circularly polarized antenna with a dual-coupled line," *IEEE Antennas and Wireless Propagation Letters*, vol. 19, no. 8, pp. 1415–1419, 2020.